Median ellipse parameterization for robust measurement of fuel droplet size

Michael Greminger and Alison Hoxie

Department of Mechanical and Industrial Engineering, University of Minnesota Duluth, 1305 Ordean CT, Duluth, MN 55812, USA

E-mail: mgreming@d.umn.edu

CrossMark

Abstract

The combustion properties of blended fuel combinations can be characterized by performing single droplet fuel combustion experiments. These combustion experiments are visualized using high speed image acquisition. Once the high speed images are obtained, the burn rate and other characteristics of combustion, such as the occurrence of microexplosions, can be characterized. Currently these quantities are either measured manually or are measured using automated software. However, the current software packages used for this task are limited in that they can only measure droplets that are elliptical in shape and manual corrections often have to be made to avoid significant errors in the measurement. An automated droplet tracking algorithm is presented that can automatically track droplet size without manual intervention due to its robustness to the presence of missing or extra edges in the images. In addition, the proposed method can track shapes more general than ellipses, which is required in order to track the droplet during microexplosions. The proposed algorithm starts by fitting ellipses to numerous five point subsets from the droplet edge data. The closed contour is parameterized by determining the median perimeter of the set of ellipses. The resulting curve is not an ellipse, allowing arbitrary closed contours to be parameterized. The performance of the proposed algorithm and the performance of existing algorithms are compared to a ground truth segmentation of the fuel droplet images. This comparison demonstrates that the median ellipse parameterization algorithm has improved performance for both area quantification and edge deviation.

Keywords: droplet size measurement, combustion, image processing, robust ellipse fitting, contour fitting

(Some figures may appear in colour only in the online journal)

1. Introduction

Burn rates of various liquid fuels can be characterized by measuring fuel droplet size versus time for a single droplet burn. A method is presented that automates the measurement of droplet area during single droplet combustion experiments. This technique is particularly efficient at accurately measuring droplet size during microexplosion events, where the droplet cannot be effectively represented by a circle or an ellipse. The proposed method is also robust to missing or extra edges in the source images. Extra edges frequently occur due to the presence of the wires that are used to suspend the droplet during the combustion experiment.

The majority of literature published on single droplet burning do not describe the technique used for determining droplet size throughout the burning process [1–3]. The most likely methods are either a manual method, where measurements are manually taken from the image as described in [4], or a method that uses commercial software to fit circles or ellipses to the droplet as described in [5]. The technique described in this paper automates this process and is shown to be more accurate as compared to commercially available motion tracking software packages. Also, the automation process allows for a more accurate burn rate measurement as the processing of higher frame rates with large numbers of images becomes feasible. In addition, the method presented here is

robust to extra features present in the image including the wires that the fuel droplets are suspended from.

The problem of determining the fuel droplet size will be reduced to that of fitting a closed contour to a set of points that represent the edge of the fuel droplet. These edge points will be obtained using a sequence of image processing operations that will be described below. Due to the presence of the wires from which the fuel droplet is suspended, some of these points will be outlier points. The proposed algorithm robustly fits a contour to this set of points even with the presence of these outlier points. The proposed algorithm will be compared to existing robust algorithms that are intended to fit ellipses to a set of points in the presence of outliers.

In the field of computer vision, ellipse fitting to data in the presence of noise and outliers continues to be an area of active research. Ahn *et al* proposed the least-squares orthogonal distance fitting method for fitting conics to data [6]. Ahn *et al*'s method is robust to normally distributed noise but outliers impact the quality of fit. Fitzgibbon *et al* developed an ellipse fitting technique that is robust to occlusion by restricting the fit to ellipses rather than all possible conics [7]. To increase the robustness of ellipse fits to outliers, methods have been developed to eliminate the outliers from the data. The most widely used method for removing outliers is the random sample consensus (RANSAC) approach to outlier rejection [8], which has also been applied to ellipse fitting by Duan *et al* [9]. Other outlier rejection schemes have also been proposed such as the two-stage outlier rejection algorithm proposed by Yu *et al* [10]. The Hough transform [11], which uses a voting approach to reject outliers, can be applied to ellipses as well [12].

An exhaustive five point ellipse fitting approach has been proposed by Rosin [13]. In Rosin's proposed approach, all combinations of five points from the data set are selected and a conic section is fit to each set of the five points. Conic sections that are not ellipses or circles are thrown out. The ellipse fit is then taken as the median parameter set (center, long axis length, short axis length, and angle) of all of the ellipses fit to the dataset. This approach performs well at rejecting outliers but has the limitation that an exhaustive ellipse fitting to all possible sets of five points in a source dataset requires $O(N^5)$ ellipse fits, where there are N points to be fit. Rosin addressed this problem by only using a uniformly spaced subset of all of the five point sets.

The curve fitting algorithm proposed here uses the multiple ellipse fitting approach of Rosin as the first stage of the algorithm. A subsampling strategy is used to limit the total number of ellipses that are fit to the data. The impact of this subsampling strategy will be characterized. This random sampling of ellipse fits is then used to parameterize the curve fit. The resulting fit is not actually an ellipse but is a median perimeter of all of the ellipses fit to the data. The unique property of the proposed algorithm is that it can fit closed contours that are more general than an ellipse while still robustly rejecting outlier points.

This article begins with a description of the proposed median ellipse parameterized algorithm in section 2. Section 3 describes the experimental facility used to capture the high speed images of the fuel droplets during combustion. Section 4 describes how the median ellipse parameterization algorithm is applied to the analysis of fuel droplets. The results are presented in section 5. Finally, section 6 contains a concluding discussion.

2. Median ellipse parameterization algorithm

The first step in the proposed median ellipse parameterization algorithm is to fit multiple ellipses to subsamples of five points from the source data set. One strategy would be to exhaustively choose all possible combinations of five points in the dataset. However, this would result in excessive computational cost for even a moderate number of data points so a random subsampling strategy will be used to fit only a fraction of the total number of five point combinations with ellipses. The impact of this ellipse subsampling will be quantified.

2.1. Ellipse fitting

Five points is the minimum number of points required to uniquely fit an ellipse. Each ellipse can be expressed in the general conic form as

$$Ax^2 + Bxy + Cy^2 + Dx + Ey + F = 0 \qquad (1)$$

where the coefficients are determined by the following equation

$$\det\left(\begin{bmatrix} x^2 & xy & y^2 & x & y & 1 \\ x_1^2 & x_1y_1 & y_1^2 & x_1 & y_1 & 1 \\ x_2^2 & x_2y_2 & y_2^2 & x_2 & y_2 & 1 \\ x_3^2 & x_3y_3 & y_3^2 & x_3 & y_3 & 1 \\ x_4^2 & x_4y_4 & y_4^2 & x_4 & y_4 & 1 \\ x_5^2 & x_5y_5 & y_5^2 & x_5 & y_5 & 1 \end{bmatrix}\right) = 0 \qquad (2)$$

and (x_i, y_i) are the five points that are used to define the ellipse. The conic section defined by (2) is not necessarily an ellipse unless it satisfies the following conditions [14]

$$B^2 2 - 4AC < 0 \qquad (3)$$

$$C\left(\left(AC - \frac{B^2}{4}\right)F + \frac{BED}{4} - \frac{CD^2}{4} - \frac{AE^2}{4}\right) < 0 \qquad (4)$$

A predetermined number of five point sets are randomly sampled from the list of points and only the five point sets that result in an ellipse are retained. Figure 1 shows a set of ellipses fit to a set of 500 points. 100 conic sections were fit to 100 random samples of 5 points taken from the 500 original points. Figure 1 shows 61 ellipses where the other 39 conics were not ellipses. In practice, 61 ellipses would not be enough to generate a good curve fit as will be seen below.

2.2. Median curve parameterization

Once the desired number of ellipses are fit to the data, the curve can now be parameterized. A polar parameterization is used for the curve. The first step in the parameterization is to locate the center of the curve fit. This is done in the manner suggested by Rosin [13] where the median center of the all of the ellipse fits
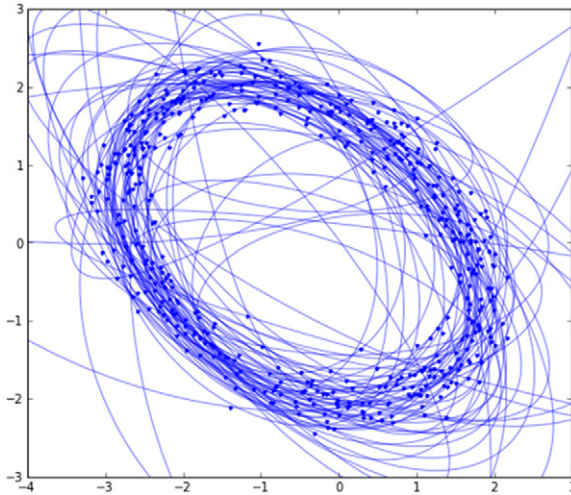
Figure 1. Ellipses fitted to subsets of five points.

is taken as the center for the polar parameterization of the curve fit. Using this center point, a ray is cast for a given angle θ. The intersections between this ray and each of the ellipses that were fit to the data are computed. Only ellipses that enclose the center point are used, which eliminates cases of multiple or no intersections. The radius of each intersection is computed and the median radius of all of the intersections is taken to be r for the current value of θ. Figure 2 shows one example of the computation of the median ellipse intersection point. Only a small number of ellipses are shown in this figure for clarity. Using the median intersection, rather than the average intersection, enables this algorithm to be robust to outliers.

Since the median point is chosen independently for every ray angle θ, a different ellipse may be chosen as the median point at different locations along the curve fit. Because of this property of the median ellipse parameterization algorithm, the resulting curve fit is not an ellipse. However, it is desirable for the median ellipse parameterization to degenerate to an ellipse when the underlying data represents an ellipse as will be illustrated below.

The median ellipse parameterization is guaranteed to have C^0 continuity since the median point will remain on a single ellipse over a range of θ until another ellipse crosses that ellipse causing the median ellipse fit to move to the next ellipse at the crossing point. However, C^1 continuity is not guaranteed since the crossing ellipses will have different slopes. Even though C^1 continuity is not enforced, it will be seen from the results that the median ellipse parameterizations are smooth due to the large number of ellipses used to generate the median ellipse parameterization.

2.3. Median ellipse parameterization applied to noisy data with and without outliers

The simplest case to test the proposed algorithm is with source data that represents an ellipse with normally distributed noise. The main purpose of this test case is to insure that the median ellipse parameterization algorithm will degenerate to an ellipse if the underlying curve is an ellipse. Figure 3 shows the noisy ellipse dataset along with an orthogonal least squares fit to the dataset based on the algorithm proposed by Ahn *et al*

[6]. Figure 3 also shows the median ellipse parameterization fit to the same noisy ellipse dataset. From figure 3, it can be seen that median ellipse parameterization algorithm performs similarly to the orthogonal least squares algorithm for the case of an ellipse with normally distributed noise. To generate the median ellipse parameterization, 10 000 conics were fit to the data with 5747 of those conics being ellipses (figure 4 shows a cloud of these 5747 ellipses).

Since only a subsample of the total number of possible conic fits are being used to generate the median ellipse parameterization, it is important to characterize the impact that this subsampling has on the fit accuracy. Over 2×10^{11} conic fits would be required to exhaustive fit all combinations of five points to a 500 point dataset. To perform this number of fits would be computationally prohibitive so only a small fraction of the total number of possible conic fits are used. Figure 5 shows the influence of the number of ellipses on the quality of the fit. The error is quantified in table 1 where the error to the true ellipse is averaged over 200 points around the circumference of the median curve fit. It can be seen from the table that for 556 or more ellipses, the error levels off to a magnitude that is only slightly higher than was obtained using an orthogonal least squares fit. This verifies that a subsampling of the possible ellipse fits can be used to generate a curve parameterization with accuracy similar to a least squares fit for the case of a noisy ellipse. When median ellipse parameterization is applied to a new problem, a similar convergence study should be performed in order to insure that a sufficient number of conics are used to generate the median curve fit.

Figure 6 shows an example of a median ellipse parameterization curve fit to a noisy ellipse in the presence of outliers. The noisy ellipse consists of 500 points and there are 100 outliers from a different ellipse. Again, 10 000 conics were fit to the data with 5209 being ellipses. It can be seen from figure 6 that the original ellipse is fit well even in the presence of a significant number of outliers which themselves are from a different ellipse. This robustness property of the median ellipse parameterization algorithm will be used below to analyze fuel droplet combustion images.

2.4. Impact of multimodality on the performance of median ellipse parameterization

As has been shown, the median ellipse intersection for the parameterization of a curve fit can handle some level of outliers in the data. However, if the distribution of ellipse intersections for each ray becomes multimodal, the median statistic will begin to fail, especially if the mode peaks in the distribution start to become comparable in size. Figure 7 shows the case where, if the number of outliers is increased to 200 points, the median ellipse parameterization fails. Using the mode rather than the median can be beneficial for cases where the distribution is multimodal. The mode for each ray is defined as the radius with the most ellipse intersections. This can be computed using a histogram of the ellipse intersection radii for each ray. However, the results using a histogram are highly dependent on the chosen bin locations and the resolution is limited by the bin width. Some of the limitations of
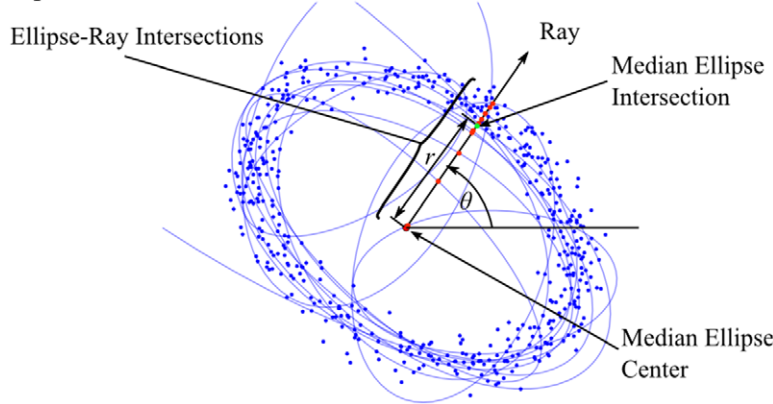
Figure 2. Calculation of curve fit radius based on the median intersection of the ellipse fits.
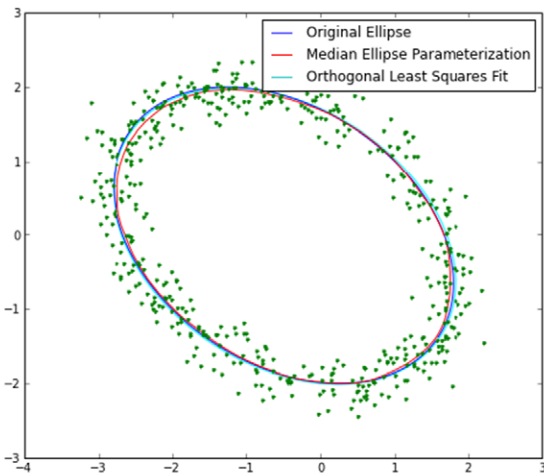

Figure 3. Noisy ellipse shown with original ellipse, orthogonal least squares fit, and the median ellipse fit.

Figure 5. Impact of the number of ellipses on the median curve fit.

Table 1. Conic fit quantity impact on the mean error.

Number of conics fit to data	Number of conics that are ellipses	Mean error (200 points)
20	12	0.116
100	53	0.038
1000	556	0.027
10 000	5603	0.031
100 000	56824	0.030
Mean error for orthogonal least squares fit		0.027

a bandwidth needs to be chosen to scale the width of the kernel. The bandwidth is analogous to the bin width for a histogram. Figure 7 shows that the mode ellipse parameterization performs well for the larger number of outliers that causes the median ellipse parameterization to fail. Figure 8 shows the KDE for one particular ray used to generate figure 7.

As discussed above, C^0 can be guaranteed with median ellipse parameterization. However, no such guarantee can be made with mode ellipse parameterization since nothing prevents the peak of the KDE of adjacent rays to swap between peaks. The performance of the median and mode ellipse parameterization will be compared for the analyses of fuel droplet images below.
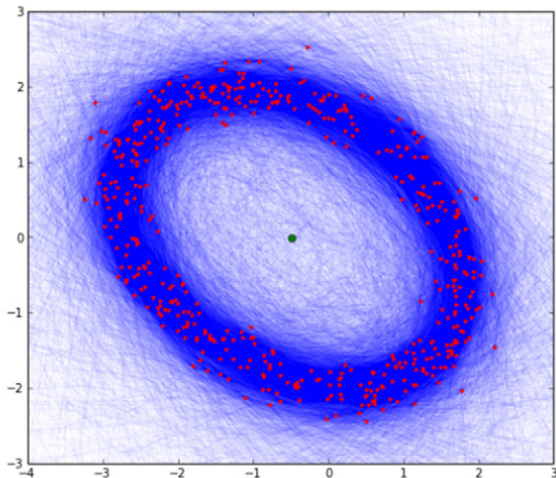

Figure 4. Ellipse cloud used to generate the median ellipse parameterization curve fit shown in figure 3.

using a histogram can be alleviated by using kernel density estimation (KDE) to estimate the probability density function of the ellipse intersection distribution [15]. A Gaussian kernel was used for the KDE results shown here. In addition,
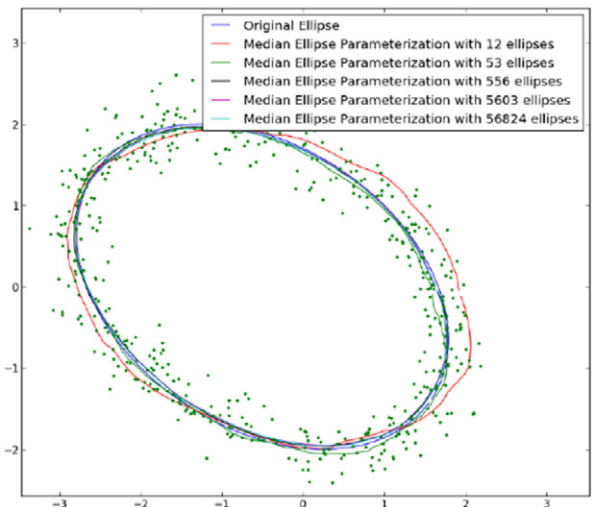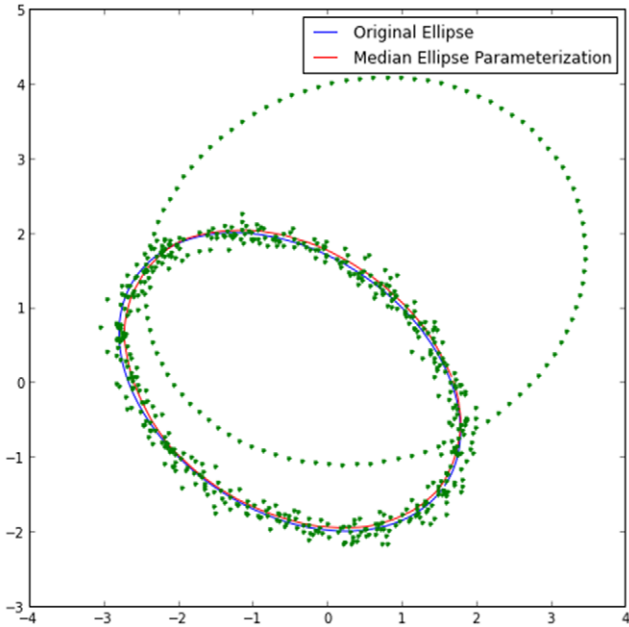
Figure 6. Median ellipse parameterization applied to an example with outliers.
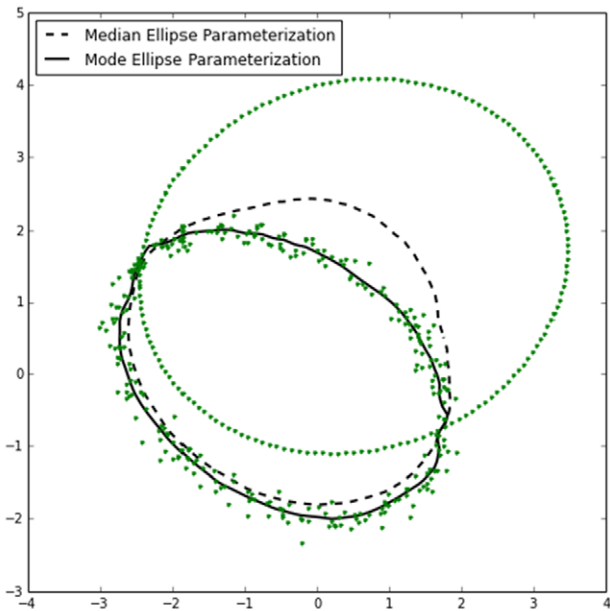

Figure 7. Median ellipse parameterization applied to an example with an increased number of outliers.

3. Droplet combustion experimental facility and procedure

Single droplet combustion experiments were conducted within a large, cubic furnace of size, $25.4 \times 25.4 \times 25.4$ cm as seen in figure 9. Two glass viewing ports, each 6.35 cm in diameter, provide visual access for an IDT NR4-S2 high-speed camera. The camera along with the Motion Studio ×64 software was used to record each trial. A 50 Watt Solar-c light box attached to the camera was used to provide adequate illumination. The furnace temperature was controlled with a Eurotherm 3504
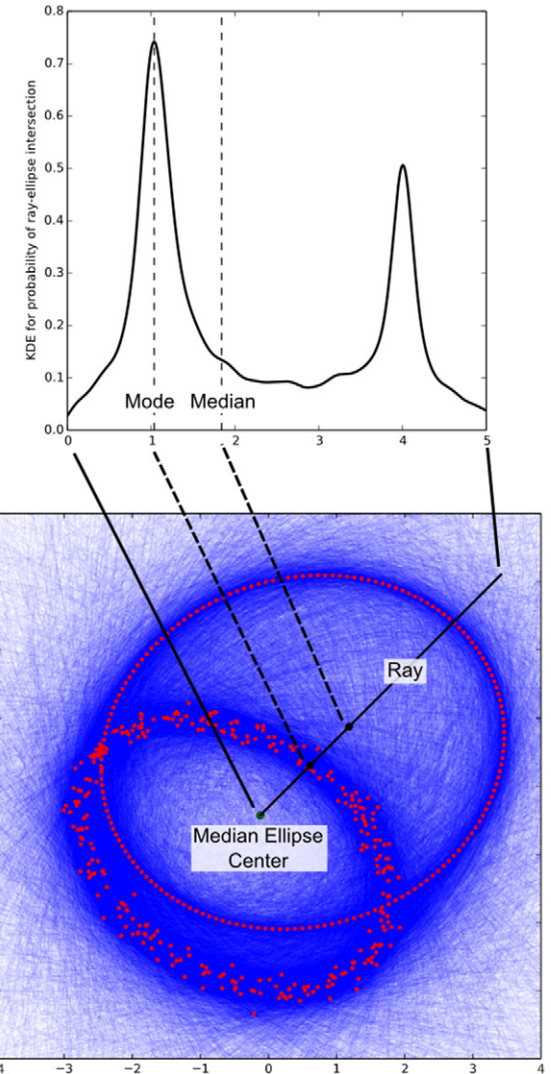

Figure 8. The ellipse cloud used to generate the fit shown in figure 7 is shown at the bottom. The kernel density estimation along a single ray is shown at the top with the median and mode locations indicated by vertical lines.

PID controller. A frame with two ceramic microfibers strung across the frame to create a perpendicular cross-section at the center was used to suspend the droplet. The microfibers have a diameter of 50 μm. Two Type K thermocouples were situated near the intersection of the microfibers, one along the side 2 mm from the droplet and one 4.5 mm directly above the droplet. The side thermocouple, with a known bead diameter of 1.3 mm, was kept in the camera's field of view for use as a size reference. The temperature readings were logged with LabView. Ignition was initiated using a resistive heating element brought close to the droplet for 0.3 s via an air controlled solenoid. For further detail on the experimental setup, the reader is referred to Shoo and Hoxie [16].

Prior to each trial, the furnace was brought to a steady-state temperature of 100 °C. The experiment was conducted at an ambient pressure of 742 mmHg. Droplets of approximately 1 mm in diameter were placed at the intersection of the microfibers using a pipette. The furnace was then lowered manually. To begin the trial, the igniter was raised to the level
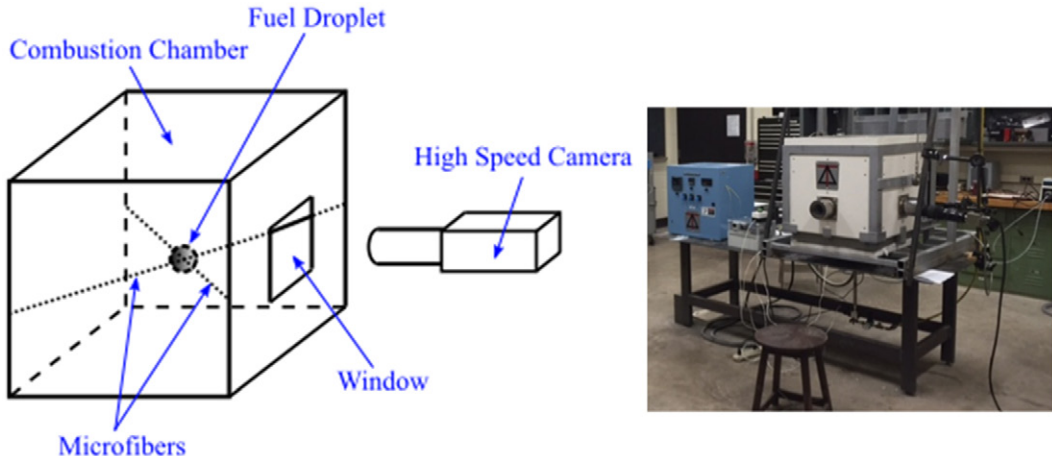
Figure 9. Droplet combustion experimental facility. A schematic is shown on the left and a photograph of the actual setup is shown on the right.

of the droplet using an air pressure system, and the heating element initiated droplet combustion. The LabView software recorded temperature of both the side and upper thermocouples at 10 times per second, and was initiated prior to lowering the furnace. This provided a quantification of the temperature disturbances due to convection within the furnace during the manual lowering process. The Motion Studio software package was set to motion trigger, and thus the camera began recording once the igniter entered the frame. The camera operated at between 300 and 400 frames per second for the duration of the droplet burn. Once the droplet had ceased to burn, the LabView program continued to record temperature data until manually stopped.

4. Median ellipse parameterization applied to the analysis of fuel droplets

As indicated above, the median ellipse parameterization algorithm takes a set of edge points as the input. Because of this requirement, the high speed images of the fuel droplets (an example of which is shown in figure 10) need to be preprocessed in order to obtain the edge points that are fed into the median ellipse parameterization algorithm as described below.

4.1. Edge point extraction algorithm

Figure 10 shows one frame from the droplet combustion image sequence. The first step in analyzing the images is to identify the location of the droplet and to take a region of interest centered around the droplet. The image is first converted to a binary image using Otsu's method [17], which is shown on the left half of figure 11. Next, the wires from which the droplet are suspended are removed from the threshold image by a specific sequence of morphological dilation and erosion operations. The resulting binary image is shown on the right half of figure 11.

The only objects that remain in the binary image are the droplet to be analyzed and the thermocouple used to monitor combustion temperature in the upper right corner of the
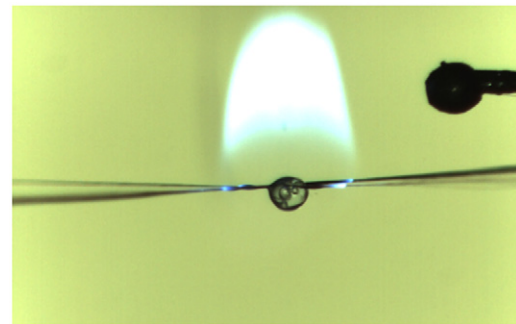

Figure 10. Burning droplet of fuel.

image. The region closest to the center of the image is taken to be the droplet region. A close-up of this droplet region is shown on the left in figure 12. The area of this region in square pixels can be used as one measure of the droplet size. This area is referred to as the morphological area in the comparisons that follow. Next, the Canny edge operator [18] is applied to the original image in the region of the droplet (see the center of figure 12). Finally, the edge points furthest from the droplet center in the radial direction are taken as the points that will be fit by the various algorithms (see the right of figure 12). It can be seen from the right of figure 12 that most of the edges have been classified correctly as the boundary of the droplet. However, at locations where the wires intersect the droplet, there are several spurious edges along with some missing edges. This misclassification of some of the edges requires that a robust algorithm is used to find the contour of the droplet.

4.2. Curve fitting results and comparison to other robust ellipse fitting algorithms

The dominant robust curve fitting algorithms can all be expressed in a framework, where, similar to the proposed algorithm and the Rosin median ellipse algorithm [13], the first step is to fit a fixed number of ellipses to randomly selected subsamples of the data points. The original RANSAC algorithm [8] used this approach to fit a model to data. In the

Figure 11. Otsu threshold image on left. Image after morphological operations on right.

Figure 12. Detected binary droplet region (left), Canny edge image of the droplet (center), and edge points used for curve fitting (right).

Table 2. Description of the algorithms compared in this article.

Algorithm	Description	Reason used
Random sample consensus (RANSAC)	Implemented by the authors based on the algorithm presented in [8]	The RANSAC algorithm is well suited to robustly fitting parameterized curves to data with a large numbers of outliers
Randomized hough transform (RHT)	Implemented by the authors based on the algorithm presented in [21]	Like the RANSAC algorithm, the RHT algorithm is another algorithm that is well suited to robustly fitting parameterized curves to data with a large numbers of outliers
Morphological area	Area obtained by quantifying the area of the binary threshold image of the droplet (see the left of figure 12)	Simplest method to quantify droplet area in an automated fashion
Ellipse fitting using the ProAnalyst software package	ProAnalyst is a commercially available image processing software	Method used previously by one of the authors for quantifying fuel droplet combustion in [16] and similar to the method used by other combustion researchers [5]
Median ellipse parameterization	Robust parameterization of the droplet perimeter using the median statistic as described in section 2	One of the new algorithms proposed in this paper
Mode ellipse parameterization	Robust parameterization of the droplet perimeter using the mode statistic as described in section 2	One of the new algorithms proposed in this paper
Manual	Manual drawing of droplet perimeter using a computer mouse	Provides the ground truth for quantifying the error of the algorithms compared in section 4.2

RANSAC algorithm, the particular curve fit from the randomly sampled points that has the most inlier points is chosen as the best fit. An orthogonal least squares fit is then made to the inlier points from this best fit. A RANSAC implementation based on the original algorithm has been implemented for the comparisons that follows.

The original Hough transform algorithm [11, 19] relied on fitting lines to all points in the image and then accumulating the two parameters that define each of the lines in a histogram. The randomized Hough transform (RHT) introduced by Xu *et al* [20] changed the original Hough transform by fitting lines to random subsamples of point pairs in the original image. In that work, Xu *et al* also devised an algorithm to implement a sparse accumulator space to alleviate the need to maintain a histogram in the parameter space for the curve to be fit. Because of the sparse accumulator, the RHT algorithm is
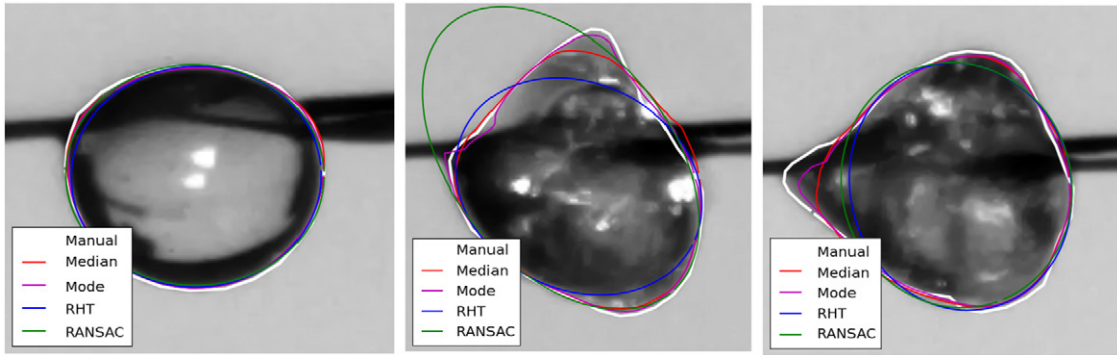
Figure 13. Three frames from the droplet combustion image sequence with curve fits. Droplet before microexplosions on the left and droplet after the initiation of microexplosions at the center and right.
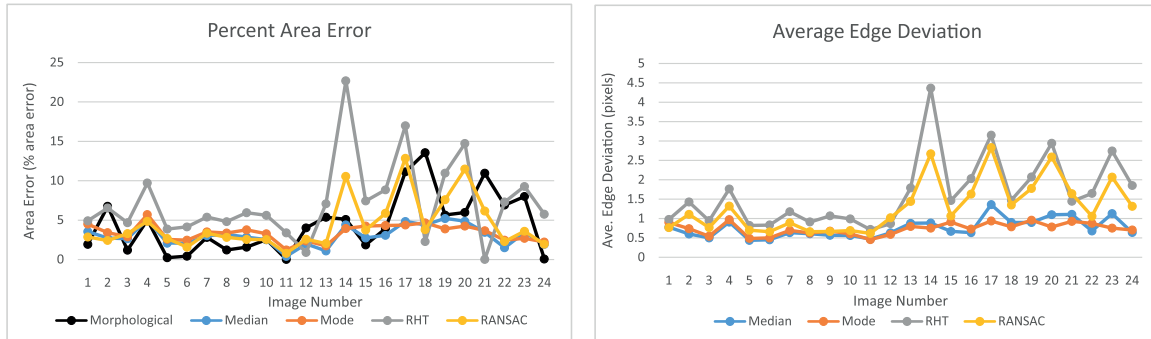

Figure 14. Fitting error for the robust contour fitting algorithms evaluated.

more suited to fitting curves with more parameters then a line, such as is the case for circles and ellipses. Xu *et al* applied their RHT algorithm to lines and circles and McLaughlin [21] expanded the algorithm to the fitting of ellipses. A RHT implementation based on the algorithm proposed by McLaughlin has been implemented for the comparison that follows.

One quantity of interest when analyzing the droplet combustion is the area of the droplet. A manual segmentation was performed on each of the 24 test images to act as the ground truth for calculating errors. One method to automatically obtain the area is to simply calculate the area of the region found using the morphological operations described above. In addition to the morphological area, the median ellipse parameterization, mode ellipse parameterization, RHT, and RANSAC algorithms were applied to the droplet combustion images. Table 2 summarizes the algorithms that are compared in the remainder of this section and in the next section.

The above procedure for finding the edge points on the boundary of the droplet was repeated for a subset of 24 images from the droplet image sequence. The curve fits, along with the manual segmentation, are shown for three of the images in figure 13. During the initial phases of combustion, the droplet is approximately elliptical and all of the algorithms have similar performance and nearly match the manual segmentation (see the left image in figure 13). However, once the microexplosions begin, the droplet shape is no longer elliptical and the ellipse based algorithms perform poorly (see the center and right images in figure 13). For these microexplosion images, the mode ellipse parameterization performs better than the median ellipse

Table 3. Average area error and average edge deviation error for robust curve fitting algorithms applied to the analysis of droplet combustion images.

	Average percent area error	Average edge deviation (pixels)
Median	3.0	0.75
Mode	3.4	0.74
RHT	7.2	1.64
RANSAC	4.3	1.30
Morphological area	4.4	

parameterization algorithm. Table 3 summarizes the average error in the area calculation for the four curve fitting algorithms and the morphological approach to area calculation. The median and mode ellipse parameterization algorithms have the lowest error when averaged across all of the images. Table 3 also quantifies the error when calculated as a radial edge deviation from the curve fit to the manual segmentation. Again, the median and mode ellipse parameterization algorithms have the lowest average edge deviation when averaged across all 24 images. These algorithms have edge deviation errors that are about half of those obtained when using the RANSAC or RHT algorithms.

Figure 14 plots both the area error and the average edge deviation versus image number for all of the images in the sequence. The images for which the RANSAC and RHT algorithms have large errors correspond to the images where microexplosions are occurring (for two examples, see the center and right hand images in figure 13).
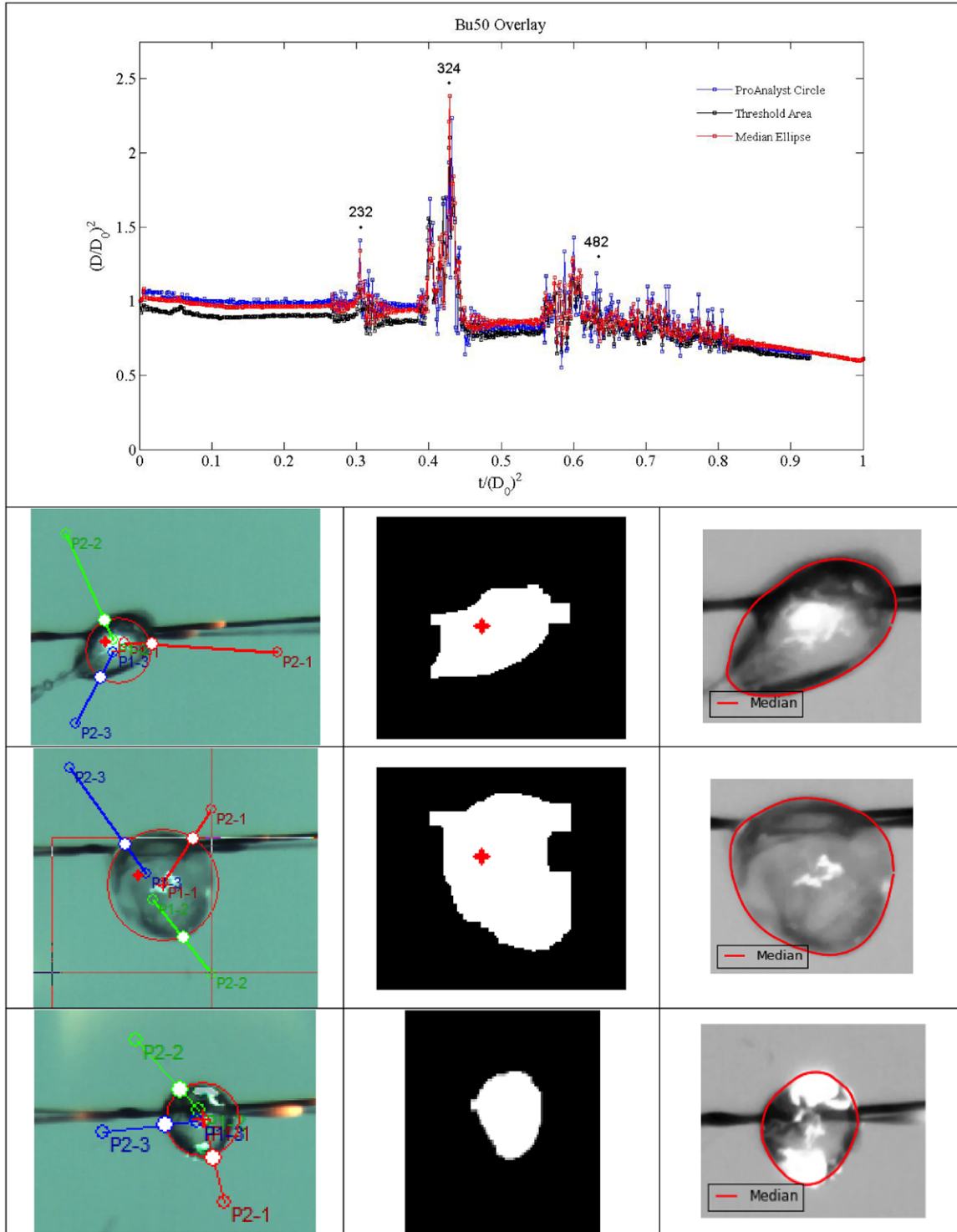
Figure 15. The left column shows the previous method used to quantify droplet size using the ProAnalyst commercial software package, the middle column shows the morphological area obtained using ProAnalyst, and the right column shows the contour obtained using the proposed median ellipse parameterization algorithm.

It can be seen from table 3 that the median ellipse parameterization algorithm has the lowest error for the area calculation and that the mode ellipse parameterization algorithm has the lowest average edge deviation. In the next section, where an entire droplet combustion sequence is analyzed, the median ellipse parameterization method will be used since the droplet area is the parameter of interest.

5. Results

In Schoo and Hoxie [16] ProAnalyst motion tracking software by Xecitex was used to measure droplet diameter as the droplet burned to completion. It provides two options for determining droplet diameter; a circle fitting algorithm and a morphological area measurement. Prior to running the algorithms the video

went through a series of processing techniques to create a binary image of just the droplet, the reader is referred to Hoxie and Schoo [16] for further detail on image processing carried out with the ProAnalyst software. ProAnalyst allows the algorithm to run through the images on its own, however both algorithms required the user to adjust the settings frequently during microexplosions in order to improve the accuracy of the fit. Figure 15 shows three cases during microexplosions of how the ProAnalyst circle, threshold area, and how the proposed median ellipse parameterization algorithm performed.

In figure 15 the left-hand column provides examples of the ProAnalyst circle fitting algorithm. For the cases shown, and for most of the images processed, the lines extending from the center of the droplet and out past its edge had to be adjusted several times in order to improve the fit of the droplet. The current image shows the best fit that could be obtained. The threshold area fit has some challenges as well. When the droplet elongates and becomes more translucent the droplet edge becomes difficult to detect, as seen in figure 15 in the middle column. Also, because the fibers that the droplets are suspended from show up dark, the threshold image algorithm picks them up. Therefore, to eliminate errors in determining the droplet area, the image needs to be cropped on the sides to eliminate the fibers. This cropping of the images needs to constantly be updated as the droplet burns and becomes smaller and also when it suddenly increases in size during microexplosions. This significantly increases the amount of time it takes to process the data since it requires an operator to continuously update the cropping window. In contrast, the proposed median ellipse parameterization algorithm is robust to the presence of the fibers so the image does not need to be manually cropped to achieve good performance. Because of this, the median ellipse parameterization algorithm can be run unsupervised allowing a very large number of images to be analyzed.

6. Discussion

Insight into the combustion characteristics of blended fuels can be obtained through single droplet combustion experiments. An important measurement needed in order to provide meaningful data is the diameter of the droplet as it burns to completion. The diameter as a function of time is determined through post-processing techniques. This paper presented an automated diameter-tracking algorithm that required little intervention by the user. This median ellipse approach was shown to be more robust to the presence of missing or extra edges in the images as compared to the morphological, commercial software, RHT and RANSAC methods. The proposed algorithm starts by fitting ellipses to numerous five point subsets from the droplet edge data. The closed curve is parameterized by determining the median perimeter of the set of ellipses. The resulting curve is not an ellipse, allowing arbitrary closed contours to be parameterized.

In addition, a combustion characteristic of importance is the microexplosion. A microexplosion causes the droplet to stretch, bubble and form various different shapes. The median ellipse algorithm was shown to track shapes more general then that of

an ellipses, therefore doing a better job of identifying the boundaries than was possible with previously used software programs. Overall, the median ellipse parameterization algorithm presented was able to identify the overall area of the droplet more accurately and with far fewer interventions by the experimentalist.

References

[1] Botero M L, Huang Y, Zhu D L, Molina A and Law C K 2012 Synergistic combustion of droplets of ethanol, diesel and biodiesel mixtures *Fuel* **94** 342–7

[2] Ikegami M, Xu G, Ikeda K, Honma S, Nagaishi H, Dietrich D L and Takeshita Y 2003 Distinctive combustion stages of single heavy oil droplet under microgravity *Fuel* **82** 293–304

[3] Xu G, Ikegami M, Honma S, Sasaki M, Ikeda K, Nagaishi H and Takeshita Y 2003 Combustion characteristics of droplets composed of light cycle oil and diesel light oil in a hot-air chamber *Fuel* **82** 319–30

[4] Esmail M, Kawahara N, Tomita E and Sumida M 2010 Direct microscopic image and measurement of the atomization process of a port fuel injector *Meas. Sci. Technol.* **21** 075403

[5] Pan K-L, Li J-W, Chen C-P and Wang C-H 2009 On droplet combustion of biodiesel fuel mixed with diesel/alkanes in microgravity condition *Combust. Flame* **156** 1926–36

[6] Ahn S J, Rauh W and Warnecke H-J 2001 Least-squares orthogonal distances fitting of circle, sphere, ellipse, hyperbola, and parabola *Pattern Recognit.* **34** 2283–303

[7] Fitzgibbon A, Pilu M and Fisher R B 1999 Direct least square fitting of ellipses *IEEE Trans. Pattern Anal. Mach. Intell.* **21** 476–80

[8] Fischler M A and Bolles R C 1981 Random sample consensus: a paradigm for model fitting with applications to image analysis and automated cartography *Commun. ACM* **24** 381–95

[9] Duan F, Wang L and Guo P 2010 RANSAC based ellipse detection with application to catadioptric camera calibration *Neural Information Processing. Models and Applications* (Berlin: Springer) pp 525–32

[10] Yu J, Zheng H, Kulkarni S R and Poor H V 2010 Two-stage outlier elimination for robust curve and surface fitting *EURASIP J. Adv. Signal Process.* **2010** 4

[11] Hough P V 1962 Method and means for recognizing complex patterns *US Patent Specification* US3069654A

[12] Cheng Y C 2006 The distinctiveness of a curve in a parameterized neighborhood: extraction and applications *IEEE Trans. Pattern Anal. Mach. Intell.* **28** 1215–22

[13] Rosin P L 1993 Ellipse fitting by accumulating five-point fits *Pattern Recognit. Lett.* **14** 661–9

[14] Mortenson M E 1997 *Geometric Modeling* 2nd edn (New York: Wiley)

[15] Silverman B W 1986 *Density Estimation for Statistics and Data Analysis* vol 26 (New York: Chapman and Hall)

[16] Hoxie A, Schoo R and Braden J 2014 Microexplosive combustion behavior of blended soybean oil and butanol droplets *Fuel* **120** 22–9

[17] Otsu N 1975 A threshold selection method from gray-level histograms *Automatica* **11** 285–96 23–7
[18] Canny J 1986 A computational approach to edge detection *IEEE Trans. Pattern Anal. Mach. Intell.* **PAMI-8** 679–98
[19] Duda R O and Hart P E 1972 Use of the Hough transformation to detect lines and curves in pictures *Commun. ACM* **15** 11–5
[20] Xu L, Oja E and Kultanen P 1990 A new curve detection method: randomized Hough transform (RHT) *Pattern Recognit. Lett.* **11** 331–8
[21] McLaughlin R A 1998 Randomized Hough transform: improved ellipse detection with comparison *Pattern Recognit. Lett.* **19** 299–305